Journal of Advances in Mathematics and Computer Science

36(8): 52-69, 2021; Article no.JAMCS.73830

ISSN: 2456-9968

(Past name: British Journal of Mathematics & Computer Science, Past ISSN: 2231-0851)

Dynamics of a Reaction Diffusion Brucellosis Model

Paride O. Lolika[1*] and Steady Mushayabasa[2]

[1] *Department of Mathematics, University of Juba, P.O.Box 82 Juba, Central Equatoria, South Sudan.*

[2] *Department of Mathematics, University of Zimbabwe, P.O.Box MP 167, Harare, Zimbabwe.*

Authors' contributions

This work was carried out in collaboration between both authors. Both authors read and approved the final manuscript.

Article Information

DOI: 10.9734/JAMCS/2021/v36i830393

Editor(s):

(1) Dr. Leo Willyanto Santoso, Petra Christian University, Indonesia.

Reviewers:

(1) Abid Sultan, University of Sargodha, Pakistan.

(2) Hamadjam Abboubakar, The University of Ngaoundéré, Cameroon.

Complete Peer review History: http://www.sdiarticle4.com/review-history/73830

Received: 24 July 2021

Accepted: 28 September 2021

Published: 07 October 2021

Original Research Article

Abstract

To understand the effects of animal movement on transmission and control of brucellosis infection, a reaction diffusion partial differential equation (PDE) brucellosis model that incorporates wild and domesticated animals under homogeneous Neumann boundary conditions is proposed and analysed. We computed the reproductive number for the brucellosis model in the absence of spatial movement and we established that, the associated model has a globally asymptotically stable disease-free equilibrium whenever the reproductive number is less or equal to unity. However, if the reproductive number is greater than unity an endemic equilibrium point which is globally asymptotically stable exists. We performed sensitivity analysis on the key parameters that drive the disease dynamics in order to determine their relative importance to disease transmission and prevalence. For the model with spatial movement the disease threshold is studied by using the basic reproductive number. Additionally we investigate the existence of a Turing stability and travelling waves. Our results shows that incorporating diffusive spatial spread does not produce a Turing instability when the reproductive number $\mathcal{R}_0^{ODE}$ associated with the ODE model is less than unity. Finally the results suggest that minimizing interaction between buffalo and cattle population can be essential to manage brucellosis spillover between domesticated and wildlife animals. Numerical simulations are carried out to support analytical findings.

**Corresponding author: E-mail: parideoresto@yahoo.com;*

Keywords: Brucellosis; reaction-diffusion; Turing stability; travelling waves; reproductive number.

2010 Mathematics Subject Classification: 53C25; 83C05; 57N16.

1 Introduction

Brucellosis remains one of the zoonotic infections of a significant public health importance, with major economic and financial burdens in countries where the disease remains endemic. More than 500 000 cases of human brucellosis occurs annually and majority of these cases have been observed in the Middle Eastern countries, southern Europe and North Africa, countries in South and Central Asia, sub-Saharan Africa, Mexico, the Caribbean, and countries in South and Central America [1].

Animal infections mostly occur due to contact with fetal tissues and post-parturient discharges, while human infections occur from contact with infected animal tissues or ingestion of infected animal products [2]. The transmission and spread of infectious disease amongst and between domesticated and wild animals is widely recognized. Factors such as seasonal variations leads to climatic changes in pastures and this induces animal movements, which in turn influence cross-infection of diseases. The effects of African buffalo movements and Zoonotic disease transmission is well documented [3].

Mathematical modeling, analysis and simulation of brucellosis play a crucial role on providing useful insight into the disease dynamics that could guide public health administration for designing effective prevention and control measures. Recently, mathematical modeling of brucellosis dynamics has been an interesting topic for a couple of researchers (see, for example [4, 5, 6, 7, 8, 9, 10, 11, 12, 13]). These studies and several other studies undeniably revealed many useful results and improved the existing knowledge on brucellosis dynamics.

Despite all these studies there are some important questions regarding the transmission of brucellosis that are yet to be answered. For example, why does brucellosis remain endemic in some countries (such as Spain, Latin America, the Middle East, parts of Africa [14]) but not in others? What is the influence of animal movements on the spread of the brucellosis? How to measure the infection risk of brucellosis in an environment where domesticated and wildlife species interact? To date very little work has been devoted to explore the influence of animal movements on brucellosis dynamics.

In 2016 Caron et al [15] presented a report on the long-distance movements of sub-adult female buffalo within a transfrontier conservation area in Africa. The authors noted that in January 2014, a 2.5 year-old female buffalo collared in South Africa walked a maximum distance of 95 km, and in 6 days, she crossed into Zimbabwe, then into Mozambique, and into Zimbabwe again. On the second incident, in February 2014, a 4-year-old female buffalo is believed to have walked a distance of 64 km in 8 days. On the third case, in March 2013, a 4.5-year-old female buffalo captured in July 2011 was sighted in a location deep into communal land at a distance of 96 km from her capture site. It is clear that animal movements could play an important role in shaping the complex epidemic and endemic pattern of brucellosis, and it is a key factor in the epidemiology of brucellosis.

Hence the goal of this paper is to improve our quantitative understanding of the effects of animal movements on brucellosis dynamics. To achieve this goal, we propose and analyse a reaction-diffusion brucellosis model that incorporates domesticated (cattle) and wildlife (African buffalo) animals. For each population, the total population is sub-divided into two epidemiological compartments namely: susceptible and infectious. We will begin by formulating and analysing a deterministic brucellosis model, which will then be extended to a reaction-diffusion PDE system to explore the effects of animal movements on the spread of brucellosis.

We will pay special attention to the travelling wave solutions and threshold dynamics of the PDE model.

The paper is organized as follows. In Section 2, the partial differential equation (PDE) model is presented and necessary assumptions are stated. In Section 3, we analyse the brucellosis model without and with diffussion, respectively. In Section 4, numerical results are carried out in order to support analytical findings. A brief discussion and conclusion in Section 5 rounds up the paper.

2 Materials and Methods

2.1 Model description

We introduce a one-dimensional spatial domain, $x \in [0, 1]$ on the assumption that both livestock and wildlife population undergo a diffusion process. We classify each population into two compartments namely, susceptible $S_i(t)$ and infectious $I_i(t)$. The subscript $i = b, c$, represent buffalo and livestock populations, respectively. Let $D_i > 0$ $(1 \leq i \leq 4)$ be the diffusion coefficients of $S_b(x,t)$, $I_b(x,t)$, $S_c(x,t)$ and $I_c(x,t)$, respectively. The model takes the form:

$$\left.\begin{array}{rcl} \dfrac{\partial S_b}{\partial t} &=& \mu_b N_b - [\beta_{bb} I_b + \beta_{cb}(1-\epsilon) I_c] S_b - \mu_b S_b + D_1 \dfrac{\partial^2 S_b}{\partial x^2}, \\ \dfrac{\partial I_b}{\partial t} &=& [\beta_{bb} I_b + \beta_{cb}(1-\epsilon) I_c] S_b - [\mu_b + d_b] I_b + D_2 \dfrac{\partial^2 I_b}{\partial x^2}, \\ \dfrac{\partial S_c}{\partial t} &=& \mu_c N_c - [\beta_{bc}(1-\epsilon) I_b + \beta_{cc} I_c] S_c - \mu_c S_c + D_3 \dfrac{\partial^2 S_c}{\partial x^2}, \\ \dfrac{\partial I_c}{\partial t} &=& [\beta_{bc}(1-\epsilon) I_b + \beta_{cc} I_c] S_c - [\mu_c + \gamma + d_c] I_c + D_4 \dfrac{\partial^2 I_c}{\partial x^2}. \end{array}\right\} \tag{1}$$

Further, we assume the entire domain represents a closed community of our interest with an assumption that, no individual would cross the boundary the only recruitment is by birth. Hence, we impose null Neumann boundary conditions for $x \in [0, 1]$ for $t > 0$:

$$\frac{\partial S_i}{\partial x} = \frac{\partial I_i}{\partial x} = 0, \quad i = b, c. \tag{2}$$

It follows that the total population at time t is $N_i(t) = S_i(t) + I_i(t)$. We assume that constant size population for each specie with a recruitment and non-brucellosis-related death rate at time t given by μ_i. In addition, we assume that natural mortality occurs in all classes at a constant rate and infectious animals suffer mortality due to infection at rate d_i. Parameter β_{ij} $(i, j = b, c)$ denotes disease transmission rate, with $i = j$ implying buffalo-to-buffalo or cattle-to-cattle transmission and $i \neq j$ signify cross-transmission, respectively. Parameter ϵ accounts for minimized interaction between wildlife and domesticated animals. Practically these account for the impact of game deterrent fences. If $\epsilon = 1$ it follows that wildlife and domesticated animals do not interact, γ denotes culling rate of domesticated animals.

3 Dynamical Behavior of the Brucellosis Model

In this section, we will perform the analysis of the proposed brucellosis model. in particular, we will begin by analyzing the dynamics of the model without spatial movements.

3.1 Model without spatial movement

In the absence of spatial movement, that is, $D_i = 0$, for $i = 1, 2, 3, 4$, system (1) becomes to

$$\left.\begin{array}{rcl} \dot{S}_b(t) &=& \mu_b N_b - [\beta_{bb} I_b + \beta_{cb}(1-\epsilon) I_c] S_b - \mu_b S_b, \\ \dot{I}_b(t) &=& [\beta_{bb} I_b + \beta_{cb}(1-\epsilon) I_c] S_b - [\mu_b + d_b] I_b, \\ \dot{S}_c(t) &=& \mu_c N_c - [\beta_{bc}(1-\epsilon) I_b + \beta_{cc} I_c] S_c - \mu_c S_c, \\ \dot{I}_c(t) &=& [\beta_{bc}(1-\epsilon) I_b + \beta_{cc} I_c] S_c - [\mu_c + \gamma + d_c] I_c. \end{array}\right\} \tag{3}$$

It can easily be verified that the domain of biological interest for system (3) is :

$$\Gamma = \left\{ (S_b, I_b, S_c, I_c) \in \Re_+^4 : S_b, I_b, S_c, I_c \geq 0, \quad N_b = S_b + I_b, \quad N_c = S_c + I_c \right\}, \tag{4}$$

which is positively invariant and attracting. It is evident that system (3) admits an infection/disease-free equilibrium given by

$$\mathcal{E}^0 : \left[S_b^0, I_b^0, S_c^0, I_c^0\right] = [N_b, 0, N_c, 0]\,.$$

One of the most important threshold parameters in infectious disease modeling is the reproductive number, which is defined as the average number of new infections generated by a single infected individual in a completely susceptible population. The reproductive number measures the power of the disease to invade the population. Based on the standard next-generation matrix technique [16] and our assumptions, matrices F and V can be written as:

$$F \;=\; \begin{bmatrix} \beta_{bb} N_b & \beta_{cb}(1-\epsilon) N_b \\ \beta_{bc}(1-\epsilon) N_c & \beta_{cc} N_c \end{bmatrix} \quad \text{and} \quad V = \begin{bmatrix} (\mu_b + d_b) & 0 \\ 0 & (\mu_c + \gamma + d_c) \end{bmatrix}. \tag{5}$$

The basic reproductive number of system (3) is the dominant eigenvalue of the next generation matrix FV^{-1},

$$\mathcal{R}_0^{ODE} \;=\; \frac{1}{2}\Big[(\mathcal{R}_{bb} + \mathcal{R}_{cc}) + \sqrt{(\mathcal{R}_{bb} - \mathcal{R}_{cc})^2 + 4\mathcal{R}_{bc}\mathcal{R}_{cb}}\,\Big], \tag{6}$$

with

$$\left.\begin{array}{rcl} \mathcal{R}_{bb} &=& \dfrac{\beta_{bb} N_b}{d_b + \mu_b}, \quad \mathcal{R}_{cc} = \dfrac{\beta_{cc} N_c}{d_c + \gamma + \mu_c}, \\ \mathcal{R}_{bc} &=& \dfrac{\beta_{bc}(1-\epsilon) N_c}{d_b + \mu_b}, \quad \mathcal{R}_{cb} = \dfrac{\beta_{cb}(1-\epsilon) N_b}{d_c + \gamma + \mu_c}. \end{array}\right\}$$

The quantities $\mathcal{R}_{ii}$ and $\mathcal{R}_{ij}$ $(i, j = b, c$, with $i \neq j)$ correspond, respectively, to the average number of secondary infections through inter-species and cross-species transmission caused by one infectious animal in its infectious lifetime.

3.1.1 Stability analysis of the model without spatial movement

The local stability of the disease-free equilibrium can be directly obtained from Theorem 2 of Van den Driessche and Watmough [16]; i.e., the disease-free equilibrium $\mathcal{E}^0$ is locally asymptotically stable if $\mathcal{R}_0^{ODE} < 1$ and unstable if $\mathcal{R}_0^{ODE} > 1$.

Theorem 3.1. *If $\mathcal{R}_0^{ODE} \leq 1$, then $\mathcal{E}^0$ is globally asymptotically stable in Γ.*

Proof. The proof is based on using a Comparison Theorem [17]. Note that the equations of the infected components in system (3) can be written as

$$\begin{bmatrix} \dot{I}_b(t) \\ \dot{I}_c(t) \end{bmatrix} \;=\; [F - V] \begin{bmatrix} I_b \\ I_c \end{bmatrix} - \begin{bmatrix} Q_{11} & Q_{12} \\ Q_{21} & Q_{22} \end{bmatrix} \begin{bmatrix} I_b(t) \\ I_c(t) \end{bmatrix},$$

where

$$\left.\begin{array}{rcl} Q_{11} & = & \beta_{bb}(S_b^0 - S_b), \quad Q_{12} = \beta_{cb}(1-\epsilon)(S_b^0 - S_b), \\ Q_{23} & = & \beta_{bc}(1-\epsilon)(S_c^0 - S_c), \quad Q_{24} = \beta_{cc}(S_c^0 - S_c), \end{array}\right\}$$

with F and V as defined in (5). Further, since $S_i \leq S_i^0$, (for all $t \geq 0$) in Γ, it follows that

$$\begin{bmatrix} \dot{I}_b(t) \\ \dot{I}_c(t) \end{bmatrix} \leq [F - V] \begin{bmatrix} I_b(t) \\ I_c(t) \end{bmatrix}. \tag{7}$$

Utilizing the fact that the eigenvalues of matrix $F-V$ all have negative real parts, it follows that the linearized differential inequality (7) is stable whenever $\mathcal{R}_0^{ODE} < 1$. Consequently, $(I_b, I_c) \to (0,0)$ as $t \to \infty$. It follows from the Comparison Theorem [17] that $(I_b, I_c) \to (0,0)$ as $t \to \infty$. Hence system (3) is asymptotic to

$$\left.\begin{array}{rcl} \dfrac{d\bar{S}_b}{dt} & = & \mu_b N_b - \mu_b \bar{S}_b, \\ \dfrac{d\bar{S}_c}{dt} & = & \mu_c N_c - \mu_c \bar{S}_c, \end{array}\right\}$$

as $t \to \infty$. Clearly, $\lim_{t\to\infty}(\bar{S}_b, \bar{S}_c) = (N_b, N_c)$. Therefore, by the theory of asymptotic autonomous semi-flow

$$\lim_{t\to\infty}(S_b, S_c) = (N_b, N_c). \tag{8}$$

This implies that $\mathcal{E}^0$ is a global attractor. □

Theorem 3.2. *If $\mathcal{R}_0^{ODE} > 1$ then system (3) has a unique endemic point, $\mathcal{E}^* = (S_b^*, S_c^*, I_b^*, I_c^*)$, which is globally asymptotically stable.*

Proof. System (3) can be written in reduced form as

$$\left.\begin{array}{l} \dot{I}_b(t) = [\beta_{bb} I_b + \beta_{cb}(1-\epsilon) I_c][N_b - I_b] - [\mu_b + d_b] I_b, \\ \dot{I}_c(t) = [\beta_{bc}(1-\epsilon) I_b + \beta_{cc} I_c][N_c - I_c] - [\mu_c + \gamma + d_c] I_c. \end{array}\right\} \tag{9}$$

One can easily verify that system (9) has the feasible region:

$$\Omega = \left\{ (I_b, I_c) \in \Re_+^2 : 0 < I_b \leq N_b, \quad 0 < I_c \leq N_c \right\}. \tag{10}$$

Denoting the right hand side of (9) by (f, g), respectively, and choosing a Dulac function $D(I_b, I_c) = \dfrac{1}{I_b I_c}$, it follows that

$$\tfrac{\partial(Df)}{\partial I_b} + \frac{\partial(Dg)}{\partial I_c} = -\left(\frac{\beta_{bb}}{I_c} + \frac{\beta_{cc}}{I_b} + \frac{\beta_{cb}(1-\epsilon)N_b}{I_b^2} + \frac{\beta_{bc}(1-\epsilon)N_c}{I_c^2} \right) < 0,$$

for all $N_i, I_i > 0$ $(i = b, c)$. Thus, system (9) does not have a limit cycle in the interior of $\Omega \in \Gamma$. Additionally, we can easily rule out homoclinic and heteroclinic orbits in Ω. Since the EE is locally asymptotically stable, it follows from Poincaré-Bendixson theorem and [18, 19] that the EE is globally asymptotically stable if $\mathcal{R}_0^{ODE} > 1$. □

3.2 Analysis of the model with spatial movement

3.2.1 Turing instability

It is known that in many reaction-diffusion equations with multiple components provoke a non-equilibrium behavior, which is known as Turing instability [20], that is, there exist conditions under which the spatially uniform steady state is stable in the absence of diffusion and can become unstable

because of diffusion. We linearize system (1) at the DFE, $(S_b^0, I_b^0, S_c^0, I_c^0)^T = (N_b^*, 0, N_c^*, 0)^T$ of the model (3) in the absence of diffusion. Introducing the new coordinates $W = (W_1, W_2, W_3, W_4)^T = (S_b - S_b^0, I_b - I_b^0, S_c - S_c^0, I_c - I_c^0)^T$, we obtain the following linear system:

$$\frac{\partial W}{\partial t} = D\frac{\partial^2 W}{\partial x^2} + JW, \tag{11}$$

where J is the Jacobian matrix of the associated ODE system evaluated at the DFE, and

$$D = \text{diag}[D_1, D_2, D_3, D_4].$$

Consider the eigenvalue problem

$$\begin{aligned} \frac{\partial^2 \psi(x)}{\partial x^2} &= -\rho\psi(x), \quad x \in (0,1) \\ \frac{\partial \psi(x)}{\partial x} &= 0, \quad x = 0, 1. \end{aligned} \tag{12}$$

It can easily be verified that the eigenvalues of the boundary value problem (12) $\rho_m = (m\pi)^2 \geq 0$ with corresponding eigenfunctions $\psi_m(x) = \cos(m\pi x)$. Now let us return to our system (11). Since the system is linear, the solution $W(x,t)$ can be written as the sum of eigenfunctions

$$W(x,t) = \sum_j a_j e^{\lambda t}\psi_j(x), \tag{13}$$

where $\psi_j(x)$ is the solution of the eigenvalue problem (12), and λ and a_j are constant. Substituting (13) into (11) yields

$$|J - \rho D - \lambda I_4| = 0, \tag{14}$$

where I_4 is a 4×4 identity matrix. Now, we investigate whether there exists ρ such that $Re(\lambda) > 0$ at DFE. Solving (14) gives

$$\left.\begin{aligned} \lambda_1 &= -\frac{(m_1+m_2)}{2} + \frac{\sqrt{(m_1-m_2)^2 + 4m_3m_4}}{2}, \\ \lambda_2 &= -\frac{(m_1+m_2)}{2} - \frac{\sqrt{(m_1-m_2)^2 + 4m_3m_4}}{2}, \\ \lambda_3 &= -(\mu_b + \rho D_1), \qquad \lambda_4 = -(\mu_c + \rho D_3), \end{aligned}\right\}$$

where

$$\left.\begin{aligned} m_1 &= (\mu_b + d_b)(1 - \mathcal{R}_{bb}) + \rho D_2, \qquad m_2 = (\mu_c + \gamma + d_c)(1 - \mathcal{R}_{cc}) + \rho D_4, \\ m_3 &= \beta_{bc}(1-\epsilon)N_c, \qquad m_4 = \beta_{cb}(1-\epsilon)N_b. \end{aligned}\right\}$$

Proposition 3.1. *If $\mathcal{R}_0^{ODE} < 1$, inclusion of diffusive spatial spread into model (3) will not produce a Turing instability.*

Proof. If $\mathcal{R}_0^{ODE} < 1$, it follows that $\mathcal{R}_{ij} < 1$, for $i = j = b, c$ thus system (1) has a unique DFE, and we can conclude that $(\mu_b + d_b)(1 - \mathcal{R}_{bb}) > 0$ and $(\mu_c + \gamma + d_c)(1 - \mathcal{R}_{cc}) > 0$. Therefore we can safely conclude that $m_i > 0$ for $i = 1, 2, 3, 4$.
Further, it follows that, $\lambda_i < 0$, $(i = 2, 3, 4)$ and the only eigenvalue that could have a sign change is λ_1. We now demonstrate that $\lambda_1 < 0$. Observe that

$$\begin{aligned} \lambda_1\lambda_2 &= m_1m_2 - m_3m_4 \\ &= (\mu_b + d_b)(1 - \mathcal{R}_{bb})\rho D_4 + (\mu_c + \gamma + d_c)(1 - \mathcal{R}_{cc})\rho D_2 + \rho^2 D_2 D_4 \end{aligned}$$

$$+(\mu_b + d_b)(\mu_c + \gamma + d_c)\Big[(1 - \mathcal{R}_{bb})(1 - \mathcal{R}_{cc}) - \mathcal{R}_{bc}\mathcal{R}_{cb}\Big] \tag{15}$$

It is clear that, the first three terms of Equation (15) are positive. By theorem (3.1), $(\mu_b + d_b)(\mu_c + \gamma + d_c)[(1 - \mathcal{R}_{bb})(1 - \mathcal{R}_{cc}) - \mathcal{R}_{bc}\mathcal{R}_{cb}]$ is a product of two eigenvalues of $J_{\mathcal{E}^0}$ at the DFE, and hence it is positive since system (3) is stable at DFE . Therefore Equation (15) clearly shows that $\lambda_1 < 0$, since the product of λ_1 and λ_2 is positive, and the fact that $\lambda_2 < 0$ it follows that $\lambda_1 < 0$. Therefore, we conclude that all eigenvalues of system (1) are negative and real and this implies that Turing instability will not occur. □

3.2.2 Disease threshold

Our goal in this section is to explore the spatial threshold dynamics of brucellosis through the intrinsic analysis of the basic reproductive number derived from PDE model (1). We will make use of the ideas presented in [21, 22] to compute the basic reproductive number of the PDE model (1). Based on these studies, the basic reproductive number $\mathcal{R}_0$ for a PDE epidemic model is defined as the spectral radius of the operator

$$L[\phi(x)] = \int_0^\infty F(x)T(t)\phi dt = F(x)\int_0^\infty T(t)\phi dt\,. \tag{16}$$

in [21] they demonstrated that

$$\int_0^\infty T(t)\phi dt = -\mathcal{B}^{-1}\phi\,, \tag{17}$$

Where $\mathcal{B} := \nabla.(d_I\nabla) - V$ and

$$L = -F\mathcal{B}^{-1}, \tag{18}$$

where F and V, are as in equation (5). Further, $T(t)$ denotes the solution semi-group for the linearized reaction-diffusion system, ϕ is the distribution of the initial infection, and d_I is the diffusion coefficient vector. For our epidemic model (1), we have

$$d_I = \text{diag}[D_2, D_4], \tag{19}$$

and,

$$\mathcal{B} = \begin{bmatrix} D_2\dfrac{\partial^2}{\partial x^2} - (\mu_b + d_b) & 0 \\ 0 & D_4\dfrac{\partial^2}{\partial x^2} - (\mu_c + \gamma + d_c) \end{bmatrix}. \tag{20}$$

To analyze the basic reproductive number of the PDE system (1), $\mathcal{R}_0^{PDE} = \rho(L)$, we proceed to calculate $\mathcal{B}^{-1}$ by solving $\mathcal{B}(\phi_1, \phi_2)^T = (y_1, y_2)^T$ subject to homogeneous Neumann boundary conditions. Let us first consider the boundary value problem

$$\begin{aligned} \mathcal{B}_1[\phi_1]: &= D_2\frac{\partial^2\phi_1}{\partial x^2} - (\mu_b + d_b)\phi_1 = y_1, \quad 0 \le x \le 1; \\ \phi_1'(0) &= 0, \quad \phi_1'(1) = 0. \end{aligned} \tag{21}$$

This problem can be easily solved by using the Laplace transform. Describe the Laplace transforms of $\phi_1(x)$ and $y_1(x)$ by $\Phi_1(s)$ and $Y_1(s)$, respectively. It yields

$$\Phi_1(s) = \frac{Y_1(s)}{D_2 s^2 - (\mu_b + d_b)} + \frac{sD_2\phi_1(0)}{D_2 s^2 - (\mu_b + d_b)}$$

The inverse Laplace transform and the convolution integral then gives

$$\phi_1(x) = \frac{1}{\sqrt{D_2(\mu_b+d_b)}}\int_0^x \sinh\left[\sqrt{\frac{\mu_b+d_b}{D_2}}(x-\tau)\right] y_1(\tau)d\tau + \phi_1(0)\cosh\left[\sqrt{\frac{\mu_b+d_b}{D_2}}x\right].$$

We differentiate ϕ_1 and applying the boundary condition $\phi_1'(1)=0$, we then obtain

$$\phi_1(0) = -\frac{1}{\sqrt{D_2(\mu_b+d_b)}\sinh\left(\sqrt{\frac{\mu_b+d_b}{D_2}}\right)}\int_0^1 \cosh\left[\sqrt{\frac{\mu_b+d_b}{D_2}}(1-\tau)\right] y_1(\tau)d\tau.$$

Therefore

$$\begin{aligned}\phi_1(x) &= \mathcal{B}_1^{-1}[y_1]\\ &= \frac{1}{\sqrt{D_2(\mu_b+d_b)}}\int_0^x \sinh\left[\sqrt{\frac{\mu_b+d_b}{D_2}}(x-\tau)\right] y_1(\tau)d\tau - \frac{\cosh\left[\sqrt{\frac{\mu_b+d_b}{D_2}}x\right]}{\sqrt{D_2(\mu_b+d_b)}\sinh\left(\sqrt{\frac{\mu_b+d_b}{D_2}}\right)}\\ &\quad\times\int_0^1 \cosh\left[\sqrt{\frac{\mu_b+d_b}{D_2}}(1-\tau)\right] y_1(\tau)d\tau. \qquad (22)\end{aligned}$$

Similarly, we can solve the boundary value problem

$$\begin{aligned}\mathcal{B}_2[\phi_2]: &= D_4\frac{\partial^2\phi_2}{\partial x^2} - (\mu_c+\gamma+d_c)\phi_2 = y_2, \quad 0\le x\le 1;\\ \phi_2'(0) &= 0, \quad \phi_2'(1)=0. \qquad (23)\end{aligned}$$

We obtain that

$$\begin{aligned}\phi_2(x) &= \mathcal{B}_2^{-1}[y_2]\\ &= \frac{1}{\sqrt{D_4(\mu_c+\gamma+d_c)}}\int_0^x \sinh\left[\sqrt{\frac{\mu_c+\gamma+d_c}{D_4}}(x-\tau)\right] y_2(\tau)d\tau - \frac{\cosh\left[\sqrt{\frac{\mu_c+\gamma+d_c}{D_4}}x\right]}{\sqrt{D_4(\mu_c+\gamma+d_c)}\sinh\left(\sqrt{\frac{\mu_c+\gamma+d_c}{D_4}}\right)}\\ &\quad\times\int_0^1 \cosh\left[\sqrt{\frac{\mu_c+\gamma+d_c}{D_4}}(1-\tau)\right] y_2(\tau)d\tau. \qquad (24)\end{aligned}$$

For notations consistency, below we will switch ϕ_1 and y_1 in equations (22) and ϕ_2 and y_2 in equation (24). Now let us focus on the eigenvalue problem $L[\phi]=\lambda\phi$, that is,

$$-F\mathcal{B}^{-1}\phi = \lambda\phi. \qquad (25)$$

By virtue of (22) and (24) we can express (25) as follows,

$$\begin{aligned}\lambda\phi_i(x) &= k_{i1}\int_0^x \sinh\left[\sqrt{\frac{\mu_b+d_b}{D_2}}(x-\tau)\right]\phi_1(\tau)d\tau + k_{i2}\cosh\left[\sqrt{\frac{\mu_b+d_b}{D_2}}x\right]\int_0^1 \cosh\left[\sqrt{\frac{\mu_b+d_b}{D_2}}(1-\tau)\right]\phi_1(\tau)d\tau\\ &\quad + k_{i3}\int_0^x \sinh\left[\sqrt{\frac{\mu_c+\gamma+d_c}{D_4}}(x-\tau)\right]\phi_2(\tau)d\tau + k_{i4}\cosh\left[\sqrt{\frac{\mu_c+\gamma+d_c}{D_4}}x\right]\\ &\quad\times\int_0^1 \cosh\left[\sqrt{\frac{\mu_c+\gamma+d_c}{D_4}}(1-\tau)\right]\phi_2(\tau)d\tau, \qquad (26)\end{aligned}$$

for $i = 1, 2$, with the coefficients

$$\left.\begin{aligned}
k_{11} &= -\frac{N_b\beta_{bb}}{\sqrt{D_2(\mu_b+d_b)}}, \quad k_{12} = \frac{N_b\beta_{bb}}{\sqrt{D_2(\mu_b+d_b)}\sinh\left(\sqrt{\frac{(\mu_b+d_b)}{D_2}}\right)}, \quad k_{13} = -\frac{N_b\beta_{cb}(1-\epsilon)}{\sqrt{D_4(\mu_c+\gamma+d_c)}},\\
k_{14} &= \frac{N_b\beta_{cb}(1-\epsilon)}{\sqrt{D_4(\mu_c+\gamma+d_c)}\sinh(\sqrt{\frac{(\mu_c+\gamma+d_c)}{D_4}})}, \quad k_{21} = -\frac{N_c\beta_{bc}(1-\epsilon)}{\sqrt{D_2(\mu_b+d_b)}},\\
k_{22} &= \frac{N_c\beta_{bc}(1-\epsilon)}{\sqrt{D_2(\mu_b+d_b)}\sinh\left(\sqrt{\frac{(\mu_b+d_b)}{D_2}}\right)}, \quad k_{23} = -\frac{N_c\beta_{cc}}{\sqrt{D_4(\mu_c+\gamma+d_c)}},\\
k_{24} &= \frac{N_c\beta_{cc}}{\sqrt{D_4(\mu_c+\gamma+d_c)}\sinh\left(\sqrt{\frac{(\mu_c+\gamma+d_c)}{D_4}}\right)}.
\end{aligned}\right\}$$

3.2.3 Travelling Wave front

An important approach to study the spatial spread of brucellosis is to investigate the travelling wave solution of model (1) and to determine the critical speed of the the traveling fronts. Let a variable $u = x - vt$ where v is the speed of the disease traveling front. Assume that $N_b = S_b + I_b$ and $N_c = S_c + I_c$ are constant. Then (1) can be written as

$$\left.\begin{aligned}
\frac{dI_b}{du} &= -\frac{1}{v}\Big[(\beta_{bb}I_b + \beta_{cb}(1-\epsilon)I_c)(N_b - I_b) - (\mu_b + d_b)I_b + D_2\frac{d^2I_b}{du^2}\Big],\\
\frac{dI_c}{du} &= -\frac{1}{v}\Big[(\beta_{bc}(1-\epsilon)I_b + \beta_{cc}I_c)(N_c - I_c) - (\mu_c + \gamma + d_c)I_c + D_4\frac{d^2I_c}{du^2}\Big].
\end{aligned}\right\} \tag{27}$$

Then the corresponding first-order ordinary differential equation with respect to the variable u of system (1) is

$$\left.\begin{aligned}
\frac{dI_b}{du} &= X,\\
\frac{dI_c}{du} &= Y,\\
\frac{dX}{du} &= \frac{1}{D_2}\Big[-vX - (\beta_{bb}I_b + \beta_{cb}(1-\epsilon)I_c)(N_b - I_b) + (\mu_b + d_b)I_b\Big],\\
\frac{dY}{du} &= \frac{1}{D_4}\Big[-vY - (\beta_{bc}(1-\epsilon)I_b + \beta_{cc}I_c)(N_c - I_c) + (\mu_c + \gamma + d_c)I_c\Big].
\end{aligned}\right\} \tag{28}$$

In what follows, we will assume that $\mathcal{R}_0^{ODE} > 1$, since our current interest is the spatial spread of brucellosis. We can easily verify that model (28) has two spatially homogeneous stationary solutions, $r_0 = (0, 0, 0, 0)$ and $r_1 = (I_b^*, I_c^*, 0, 0)$. The equilibria r_0 and r_1 correspond to the disease-free and endemic equilibrium points of the ODE model (28) respectively. More specifically any traveling wave solution of (28) can be regarded as a heteroclinic orbit (minimum wave speed) connecting the disease-free equilibrium to the endemic equilibrium.

The Jacobian matrix $\mathcal{J}$ associated with the linearized system (28) evaluated at r_0 must be real for a wave front to exist. Direct calculation gives

$$\mathcal{J} = \begin{bmatrix} 0_2 & I_2 \\ \mathcal{J}_{21} & \mathcal{J}_{22} \end{bmatrix},$$

where 0_2 is the 2×2 zero matrix, I_2 denotes 2×2 identity matrix. Further

$$\mathcal{J}_{21} = \begin{bmatrix} B_{11} & B_{12} \\ B_{21} & B_{22} \end{bmatrix},$$

with

$$\left.\begin{array}{rcll} B_{11} & = & \dfrac{1}{D_2}[-\beta_{bb}N_b + (\mu_b + d_b)], & B_{12} = -\dfrac{\beta_{cb}(1-\epsilon)N_b}{D_2}, \\ B_{21} & = & -\dfrac{\beta_{bc}(1-\epsilon)N_c}{D_4}, & B_{22} = \dfrac{1}{D_4}[-\beta_{cc}N_c + (\mu_c + \gamma + d_c)], \end{array}\right\}$$

and

$$\mathcal{J}_{22} = \text{diag}\left[-\frac{v}{D_2}, \quad -\frac{v}{D_4}\right].$$

The characteristics equation of matrix $\mathcal{J}$ is

$$\lambda^4 + a_1\lambda^3 + a_2\lambda^2 + a_3\lambda + a_4 \quad = \quad 0, \tag{29}$$

where

$$\left.\begin{array}{rcl} a_1 & = & \dfrac{v}{D_2} + \dfrac{v}{D_4}, \\ a_2 & = & -\left[\dfrac{(\mu_b + d_b) - \beta_{bb}N_b}{D_2}\right] - \left[\dfrac{(\mu_c + \gamma + d_c) - \beta_{cc}N_c}{D_4}\right] + \dfrac{v^2}{D_2D_4}, \\ a_3 & = & \left[\beta_{bb}N_b - (\mu_b + d_b) + \beta_{cc}N_c - (\mu_c + \gamma + d_c)\right]\dfrac{v}{D_2D_4}, \\ a_4 & = & \left[(\mu_b + d_b) - \beta_{bb}N_b\right]\left[(\mu_c + \gamma + d_c) - \beta_{cc}N_c\right]\dfrac{1}{D_2D_4} - \dfrac{\beta_{cb}\beta_{bc}(1-\epsilon)^2N_bN_c}{D_2D_4} \\ & = & \dfrac{(\mu_b + d_b)(\mu_c + \gamma + d_c)}{D_2D_4}\left[(1 - R_{bb})(1 - R_{cc}) - R_{bc}R_{cc}\right]. \end{array}\right\}$$

The critical value of v occurs only if the characteristic equation (29) has repeated real roots. Let's consider the roots of the characteristic equation

$$p(\lambda) = \lambda^4 + a_1\lambda^3 + a_2\lambda^2 + a_3\lambda + a_4.$$

Define

(C1) $R_{cc} \leq 1$, when $\mathcal{R}_0^{ODE} > 1$;

(C2) $R_{cc} > 1$ and $R_{bb} \leq 1$;

(C3) $R_{cc} > 1$, $R_{bb} > 1$ and $(1 - R_{bb})(1 - R_{cc}) < R_{bc}R_{cc}$.

It follows from direct calculation that $a_4 < 0$ iff one of three conditions (C1)-(C3) holds. Assume that (C1), (C2) or (C3) is satisfied. Then the characteristic polynomial (29) has at least one positive and one negative zeros. We now proceed to find the condition for repeated roots. According to Jury and Mansour [23], the quartic polynomial $p(\lambda)$ undergoes the double zeros if

$$\Delta = 4A^3 - B^2 = 0, \tag{30}$$

with

$$\begin{array}{l} A = a_2^2 + 12a_4 - 3a_1a_3, \\ B = 72a_2a_4 + 9a_1a_2a_3 - 2a_2^3 - 27a_3^2 - 27a_4a_1^2. \end{array} \tag{31}$$

Assume that $D_2, D_4 > 0$. Equation (30) takes the form

$$b_1(v^2)^4 + b_2(v^2)^3 + b_3(v^2)^2 + b_4(v^2) + b_5 = 0, \tag{32}$$

where the coefficients depend on the model parameters. Specifically,

$$b_1 = \Big[\big((\mu_b+d_b)(1-R_{bb})-(\mu_c+\gamma+d_c)(1-R_{cc})\big)^2 + 4(\mu_b+d_b)(\mu_c+\gamma+d_c)R_{bc}R_{cb}\Big]\frac{(D_2-D_4)^2}{16D_2D_4} \geq 0.$$

This implies that $b_1 > 0$ when $D_2 \neq D_4$. On the other hand,

$$b_5 = \Big[\big((\mu_c+\gamma+d_c)(1-R_{cc})D_2-(\mu_b+d_b)(1-R_{bb})D_4\big)^2 + 4(\mu_b+d_b)(\mu_c+\gamma+d_c)R_{bc}R_{cb}D_2D_4\Big]^2 \times(\mu_b+d_b)(\mu_c+\gamma+d_c)\Big[(1-R_{bb})(1-R_{cc})-R_{bc}R_{cb}\Big].$$

Note that $b_5 < 0 \iff a_4 < 0$. Since (C1), (C2) or (C3) is valid, 0, we have $b_5 < 0$. Thus, in terms of v^2, equation (32) has a least one positive zero. In other words, this equation has at least a pair of real roots with respect to v which have the same magnitude and the opposite signs.

4 Numerical Results

In this section, we present numerical simulations of our study, in order to illustrate our theoretical results, using the parameters listed in Table 1.

Table 1. Parameters and values

Symbol	Value	Units
γ	0.15	year^{-1}
ϵ	0.5	Unitless
μ_b	0.04	year^{-1}
μ_c	0.22	year^{-1}
β_{bb}	5.0×10^{-4}	buffalo^{-1}year^{-1}
β_{bc}	5.0×10^{-4}	cattle^{-1}year^{-1}
β_{cc}	1.48×10^{-5}	cattle^{-1}year^{-1}
β_{cb}	1.48×10^{-5}	buffalo^{-1}year^{-1}
d_b	0.05	year^{-1}
d_c	0.15	year^{-1}
D_1	varied	km^2 d^{-1}
D_2	varied	km^2 d^{-1}
D_3	varied	km^2 d^{-1}
D_4	varied	km^2 d^{-1}
N_b	1000	Buffaloes
N_c	1500	Cattle

4.1 Sensitivity analysis of the reproductive number

The reproductive number is an integral threshold quantity for infectious disease models. It demonstrates the power of the disease to invade the community. In order to determine how best the spread of brucellosis can be controlled in a community where cattle and buffaloes interact, it is essential to know the relative importance of the different factors that make up the basic reproductive number. The reproductive number of the proposed model, equation (6), , $\mathcal{R}_0^{ODE}$, is made up of the quantities

$\mathcal{R}_{bb}$, $\mathcal{R}_{cc}$, $\mathcal{R}_{bc}$, and $\mathcal{R}_{cb}$, which represents disease transmission between buffalo to-buffalo, cattle-to-cattle, buffalo-to-cattle and cattle to buffalo, respectively. Hence, there is need to investigate which of the four aforementioned quantities has more influence on the magnitude of the reproductive number. We computed the four quantities using parameter values in Table 1.

Results in Table 2 shows that the reproductive number is greatly influenced by infectious buffalo population since $\mathcal{R}_{bb} > 1$ and $\mathcal{R}_{bc} > 1$ while $\mathcal{R}_{cc} < 1$ and $\mathcal{R}_{cb} < 1$. Therefore in a population were buffaloes interact with cattle one can conclude that the infected buffalo population will be responsible for the persistence of the disease. In addition, one can also deduce that brucellosis infection will persist in communities where the probability of livestock interaction with buffaloes is $0.5\ (1-\epsilon)$.

Table 2. Reproductive numbers and their values

$\mathcal{R}_0^{ODE}$	$\mathcal{R}_{bb}$	$\mathcal{R}_{cc}$	$\mathcal{R}_{bc}$	$\mathcal{R}_{cb}$
5.558	5.556	0.043	4.167	0.142

Results in Table 2 warrants the need to identify parameters which strongly influence $\mathcal{R}_{bb}$ and $\mathcal{R}_{bc}$ since these are the two threshold quantities greatly influencing $\mathcal{R}_0^{ODE}$. Thus we computed the sensitivity indices of the reproductive number, $\mathcal{R}_0^{ODE}$, following the approach in Arriola [24]. Sensitivity indices enables the researcher to measure the relative change in a state variable when a parameter changes. To this end, denoting by Φ the generic parameter of equation (6), we evaluate the *normalised sensitivity index* $S_\Phi = \frac{\Phi}{\mathcal{R}_{bb}} \frac{\partial \mathcal{R}_{bb}}{\partial \Phi}$, which indicates how sensitive $\mathcal{R}_0$ is to a change of parameter Φ. Model parameters with positive index increase the value of reproductive number whenever they are increased while those with a negative index decrease the value of reproductive number whenever they are increased.

Fig. 1 shows the sensitivity index for $\mathcal{R}_{bb}$ with respect to model parameters that define it. As one can observe, an increase in the values of β_{bb} and N_b by 10% will increase $\mathcal{R}_{bb}$ by the same magnitude. However, an increase in μ_b and d_b by 10% decrease $\mathcal{R}_{bb}$ by 4.44% and 5.5%, respectively.

Fig. 2 shows the sensitivity index for $\mathcal{R}_{bc}$ with respect to model parameters that define it. We can observe that, an increase in the values of β_{bb} and N_c by 10% will increase $\mathcal{R}_{bc}$ by the same magnitude while an increase in μ_b, d_b and ϵ by 10% decrease $\mathcal{R}_{bb}$ by 4.44%,5.5% and 10%, respectively. The results suggest that minimizing interaction between buffalo and cattle population can be essential to manage brucellosis spillover between domesticated and wildlife animals. Hence, in Fig. 3 we investigate the minimization level ϵ sufficient to make $\mathcal{R}_{bc} \leq 1$. Results in Fig. 3 shows that $\epsilon = 0.9$ will be sufficient to confine disease to wildlife population, since $\mathcal{R}_{bc} \leq 1$ for all $\epsilon \in [0.9, 1]$.

In Fig. 4 we examine the impact of low cross-transmission rate ($\beta_{cb} = \beta_{bc} = 0.45 < 1$) on the spread of the disease in the community. We can observe that whenever $\mathcal{R}_{cc} \leq 1$ and $\mathcal{R}_{bb} \leq 1$ the disease will die out in the community and for the reverse case the disease will persist.

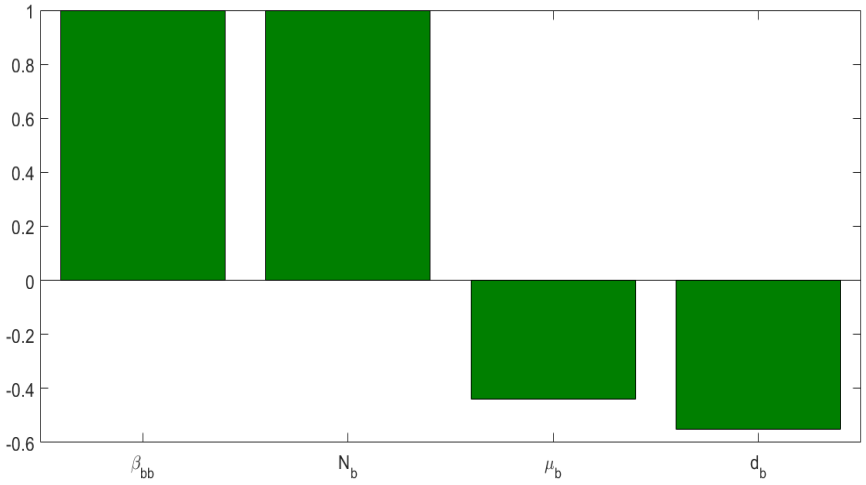

Fig. 1. Sensitivity index for $\mathcal{R}_{bb}$ with respect to model parameters that define it

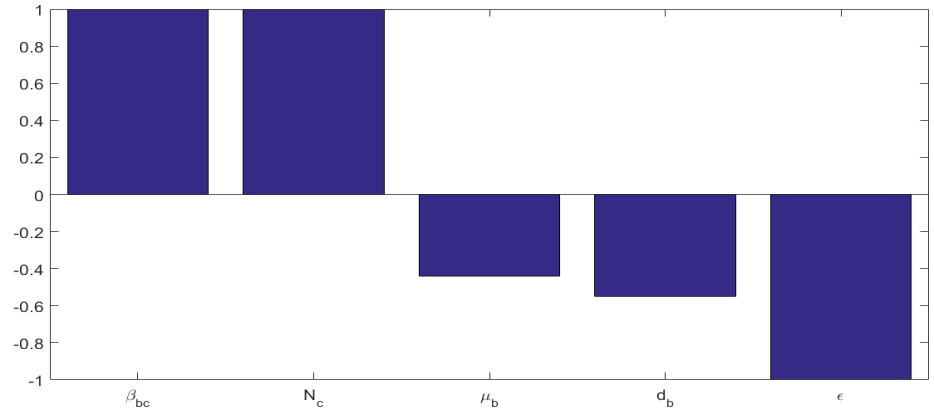

Fig. 2. Sensitivity index for $\mathcal{R}_{bc}$ with respect to model parameters that define it

Fig. 5 illustrates the effects of high cross transmission rate on the prevalence of brucellosis. For this case, on can observe that cross-transmission is high than local transmission then the disease will persist for even small values of the reproductive number.

Fig. 6 depicts the impact of varying the control parameter ϵ and the cross-transmission rate ($\beta_{cb} = \beta_{bc}$, on the spread of the disease in the community. As we can observe, if $0.5 \leq \epsilon \leq 1$ and $0 \leq \beta_{cb} \leq 1$, then brucellosis dies out in the community and for the reverse it will persist.

In Figs. 7 and 8, we illustrate the effects of the reproductive number on brucellosis dynamics, with and without spatial movement. Here we observe that that when $\mathcal{R}_0^{PDE} > 1$ then system (1) has an endemic equilibrium point with peak values occurring approximately 30 days from the start

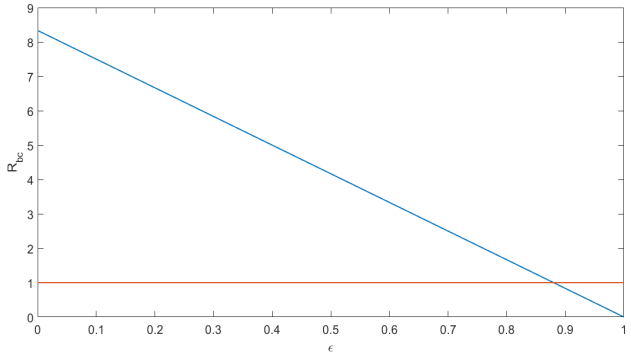

Fig. 3. Impact of controlled interaction between buffalo and livestock on transmission of brucellosis

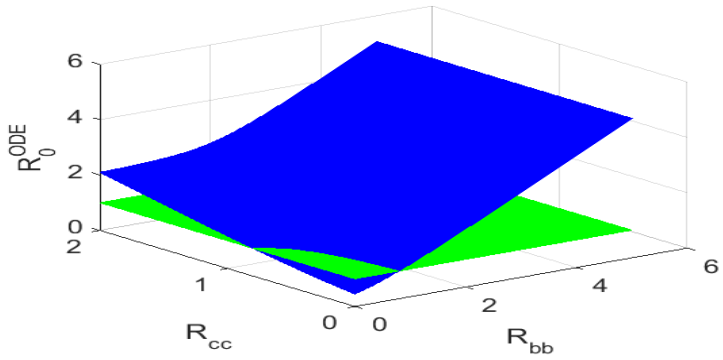

Fig. 4. Effects of low cross-transmission ($\mathcal{R}_{cb} = \mathcal{R}_{bc} = 0.45 < 1$) on transmission of brucellosis

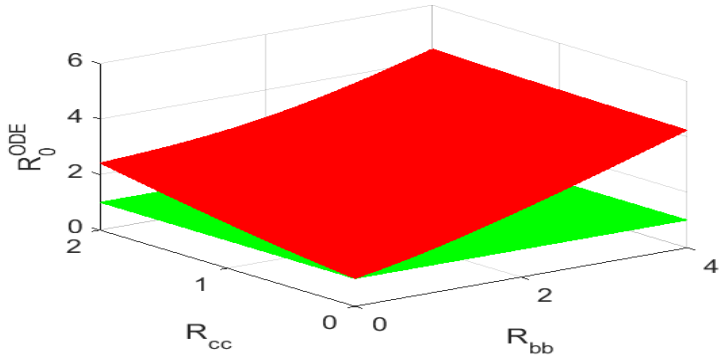

Fig. 5. Effects of high cross-transmission ($\mathcal{R}_{cb} = \mathcal{R}_{bc} = 1.05 < 1$) on transmission of brucellosis

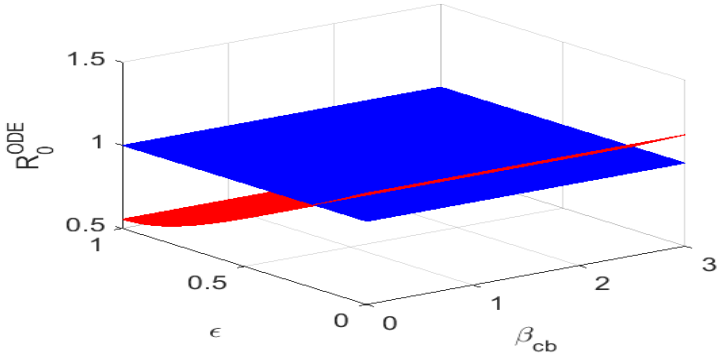

Fig. 6. Effects of varying ϵ and β_{cb} on the reproductive number $\mathcal{R}_0^{ODE}$

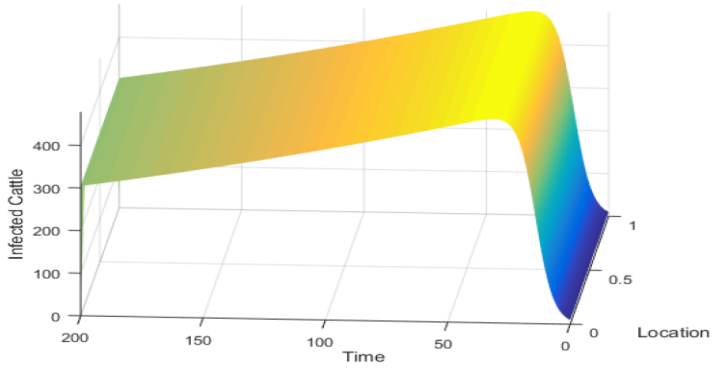

Fig. 7. Number of infected cattle associated with system (1) versus space and time when $\mathcal{R}_0^{PDE} > 1$.

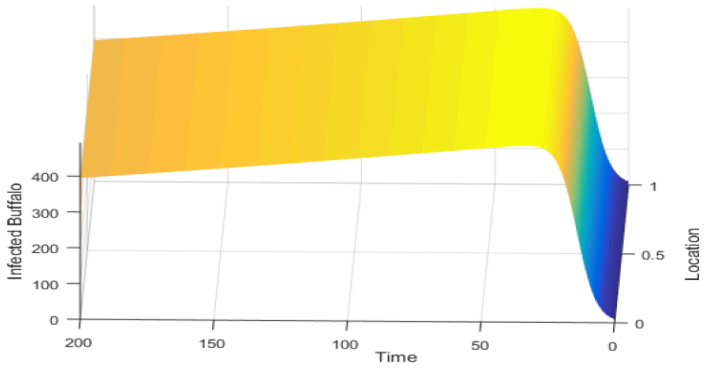

Fig. 8. Number of infected buffaloes associated with system (1) versus space and time when $\mathcal{R}_0^{PDE} > 1$.

5 Discussion and Conclusions

Many wildlife species are known to be reservoirs of zoonotic infections. In developing nations mixing of wildlife and domesticated animals is almost homogeneous since the game reserve fencing materials are seriously dilapidated. To investigate how the effects of movements of wildlife and domesticated animals lead to cross-infection of diseases and impact the spread and control of brucellosis transmission, we constructed a reaction-diffusion brucellosis model, that comprise cattle and African buffaloes. We established that without spatial animal movement, the associated model admits two equilibrium points; the disease-free and endemic. Utilizing the Comparison Theorem, we have shown that the disease-free equilibrium is globally asymptotically stable whenever the reproductive number $\mathcal{R}_0^{ODE}$ is less or equal to unity, and if the reproductive number is greater than unity there exists an endemic equilibrium which is globally asymptotically stable. Analysis for our model that constitute spatial animal movements demonstrates that incorporating diffusive spatial spread does not produce a Turing instability when $\mathcal{R}_0^{ODE} < 1$. With the aid of numerical simulations we have shown that both with and without spatial movement the disease persists whenever the associated reproductive number is greater than unity. The results also suggest that minimizing interaction between buffalo and cattle population can be essential to manage brucellosis spillover between domesticated and wildlife animals.

Finally, Several avenues for future research arise from this work. First, future research should assess the role of spatial animal movements and seasonal variation on the persistence of brucellosis, since factors such as seasonal variations leads to climatic changes in pastures and this induces animal movements. Seasonal availability of water and pastures have a significant influence on pastoral farming, hence there is need to investigate its impact on the persistence of brucellosis. Second, although we were able to establish the existence of a Turing stability and travelling waves analytically, we did not resolve the results numerically and that remains an interesting topic for our future research.

Data Availability Statement

The data used to support the findings of this study are included within the article.

Acknowledgement

The authors thank Dr. Xueying Wang and Dr. Chairat Modnak for their invaluable discussions and comments during the preparation of this manuscript. Dr. Paride O. Lolika acknowledges and thanks the support from Dr. Mohamed Y. A. Bakhet and his colleagues.

Competing Interests

Authors have declared that no competing interests exist.

References

[1] Potter EM. Brucellosis: A chapter in Foodborne infections and intoxication, 4th Edition, Morris J. G and Potter E. M (eds), Elsevier Inc; 2013.

[2] Alexander KA, Blackburn JK, Vandewalle ME, Pesapane R, Baipoledi Ek, et al. Buffalo, bush meat, and the Zoonotic threat of brucellosis in Botswana. PLoS ONE. 2012;7(3):e32842. DOI: 10.1371/journal.pone.0032842.

[3] Caron A, Cornelis D, Foggin C, Hofmeyr M, Garine-Wichatitsky M. African buffalo movement and Zoonotic disease risk across transfrontier conservation areas, Southern Africa. Emerging Infectious Diseases. 2016;22(2).

[4] Hou Q, Sun X, Zhang, Liu Y, Wang Y, Jin Z. Modeling the transmission dynamics of sheep brucellosis in Innner Mongolia autonous region, China. Mathematical Biosciences. 2013;242:51-58.

[5] Zhang J, Sun G-Q, Sun X-D, Hou Q, Li M, et al. Prediction and control of brucellosis transmission of dairy cattle in Zhejiang Province, China. PloS ONE. 2014;9(11):e108592. DOI:10.1371/journal.pone.0108592

[6] Li M, Sun G, Wu Y, Zhang J, Jin Z. Transmission dynamics of multi-broup brucellosis model with mixed cross infection in public farm. Applied Mathematics and Computation. 2014;237:582-594.

[7] Li M, Sun G, Zhang J, Jin Z, Sun X, Wang Y, Huang B, Zheng Y. Transmission dynamics and control for brucellosis model in Hingaan League Inner Mongolia, China. Mathematical Biosciences and Engineering. 2014;11:1115-1137.

[8] Lolika OP, Modnak C, Mushayabasa S. On the dynamics of brucellosis infection in bison population with vertical transmission and culling, Mathematical Biosciences. 2018;305:42-54.

[9] Lolila OP, Mushayabasa S. On the role of short-term animal movements on the persistence of brucellosis. Mathematics. 2018;6:154.

[10] Lolika OP, Mushayabasa S. Dynamics and stability analysis of a brucellosis model with two discrete delays. Discrete Dynamics in Nature and Society; 2018. Article ID 6456107, 20 pages.

[11] Lolika OP, Mushayabasa S, Bhunu CP, Modnak C, Wang J. Modeling and analyzing the effects of seasonality on brucellosis infection; Chaos, Solitons and Fractals. 2017;104:338-349.

[12] Chayu Yang, Paride O. Lolika, Steady Mushayabasa, Jin Wang. Modeling the spatiotemporal variations in brucellosis transmission. Nonlinear Analysis: Real World Applications. 2017;38:49-67.

[13] Abath E, Ron L, Speybroeck N, Williams B, Berkvens D. Mathematical analysis of the transmission dynamics of brucellosis among bison. Mathematical Methods in the Applied Sciences. 2015;38:3818-3832.

[14] Pappas G, Akritidis N, Bosikovski M , Tasianos E, Brucellosis, N. Engl. J. Med. 2005;352:2325.

[15] Caron A, Cornelis D, Foggin C, et al. African buffalo movement and zoonotic disease risk across transfrontier conservation areas, southern Africa. Emerging Infectious Diseases. 2016;22:277-280.

[16] Van den Driessche P, Watmough J. Reproduction numbers and sub-threshold endemic equilibria for the compartmental models of disease transmission. Math. Biosci. 2002;180:29-48.

[17] Lakshmikantham V, Leela S, Martynyuk AA. Stability analysis of nonlinear systems. Marcel Dekker, Incl; 2010.

[18] Nkamba LN, Ntaganda JM, Abboubakar H, Kamgang JC, Castelli L. Global stability of a SVEIR epidemic model: Application to poliomyelitis transmission dynamics. Comput. Math. Appl. 2017;5:98-112.

[19] Jin-Qiang Zhao, Ebenezer Bonyah, Bing Yan, Muhammad Altaf Khan, K.O. Okosun, Mohammad Y. Alshahrani, Taseer Muhammad,A mathematical model for the coinfection of Buruli ulcer and Cholera, Results in Physics. 2021;29:104746.
ISSN: 2211-3797.
Available:https://doi.org/10.1016/j.rinp.2021.104746

[20] Turing A. The chemical basis morphogenesis. Philos. Trans. Roy. Soc. 1952;B.237:37-72.

[21] Wang W, Zhao XQ. Basic reproduction numbers for reaction-diffusion epidemic models. SIAM J. Appl. Dyn. S. 2012;11:1652-1673.

[22] Hsu SB, Wang FB, Zhao XQ. Global dynamics of zooplankton and harmful algae in flowing habitats. J. Differ. Equations. 2013;255:3-10.

[23] Jury EI, Mansour M. Positivity and nonnegativity conditions of a quartic equation and related problems. IEEE Trans. Automat. Control, AC. 1981;26:444-451.

[24] Arriola L. Sensitivity analysis for quantifying uncertainty in mathematical models. Mathematical and Statistical Estimation Approaches in Epidemiology, G. Chowell, J.M. Hyman, L.M.A. Bettencourt, and C. Castillo-Chavez, eds., Springer, New York. 2009;195248.

Peer-review history:
The peer review history for this paper can be accessed here (Please copy paste the total link in your browser address bar)
http://www.sdiarticle4.com/review-history/73830